Inorganic Chemistry

pubs.acs.org/IC

Article

Heterometallic Au(I)−Cu(I) Clusters: Luminescence Studies and $^1O_2$ Production

Guillermo Romo-Islas, Jas S. Ward, Kari Rissanen, and Laura Rodríguez*

Cite This: https://doi.org/10.1021/acs.inorgchem.3c00046

Read Online

ACCESS | Metrics & More | Article Recommendations | Supporting Information

ABSTRACT: Two different organometallic gold(I) compounds containing naphthalene and phenanthrene as fluorophores and 2-pyridyldiphenylphosphane as the ancillary ligand were synthesized (compounds 1 with naphthalene and 2 with phenanthrene). They were reacted with three different copper(I) salts with different counterions (PF_6^-, OTf^-, and BF_4^-; OTf = triflate) to obtain six Au(I)/Cu(I) heterometallic clusters (compounds **1a−c** for naphthalene derivatives and **2a−c** for phenanthrene derivatives). The heterometallic compounds present red pure room-temperature phosphorescence in both solution, the solid state, and air-equilibrated samples, as a difference with the dual emission recorded for the gold(I) precursors **1** and **2**. The presence of Au(I)−Cu(I) metallophilic contacts has been identified using single-crystal X-ray diffraction structure resolution of two of the compounds, which play a direct role in the resulting red-shifted emission with respect to the gold(I) homometallic precursors. Polystyrene (PS) and poly(methyl methacrylate) (PMMA) polymeric matrices were doped with our luminescent compounds, and the resulting changes in their emissive properties were analyzed and compared with those previously recorded in the solution and the solid state. All complexes were tested to analyze their ability to produce $^1O_2$ and present very good values of Φ_Δ up to 50%.

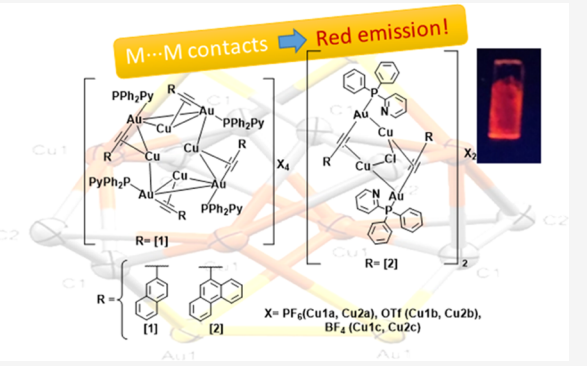

INTRODUCTION

Polydentate ligands are one of the most employed methods to generate complexes with a large number of atoms in their structure.[1−4] The chemical structure of these ligands can be modified to include different donor atoms, and following this strategy, a wide variety of metallic clusters, polymers, aggregates, and supramolecular structures have been reported in the literature.[5−8] Among polydentate ligands, the use of pyridylphosphane seems an ideal choice for the construction of heterometallic structures derived from group 11 elements due to their tendency to coordinated Au(I) through the phosphorus atom and to Ag(I) or Cu(I) through nitrogen centers. The presence of additional ancillary ligands such as acetylide groups may also favor the coordination of Ag(I) or Cu(I), promoting the formation of complex heterometallic assemblies.[9−11]

Metallic centers with closed-shell d^{10} electronic configurations have a tendency to form metallophilic (metal···metal) interactions. These interactions play an important role in the luminescent properties of the compounds, giving as a result compounds with different applications, for example, as luminescent materials with different colors such as blue[12] green,[13] red,[14] or white emissions,[15] thermally activated delayed fluorescence (TADF) systems,[10,16−18] or as sensors[19−21] among others. These applications depend not only on the metallophilic contacts but also on their ligands, where polydentate ligands play an important role in facilitating metal···metal proximity. Among d^{10} metallic compounds, gold(I) complexes bearing alkynyl moieties bonded to polyaromatic fluorophores have been demonstrated to be highly emissive.[22−25] The emission of these systems is often related to the presence of aurophilic interactions and the formation of aggregates with high nuclearity.[26−32] These interactions modify the electronic structure of the systems favoring the appearance of cluster-centered (CC) and metal−metal-to-ligand charge-transfer (MMLCT) emissive transitions.[27,33] Additionally, intramolecular metal···metal interactions can be promoted by using polydentate ligands.[29] Different donor atoms in these ligands can coordinate to several metal centers, keeping them close to each other and establishing heterometallic metallophilic interactions. Thus, the inclusion of a second metal ion, such as Ag(I) or Cu(I), in Au(I) complexes with multidentate ligands may promote the formation of cluster structures.[34−36] These structures generate a change in the emission spectra of compounds following diverse processes such as CC, MMLCT, or LMMCT caused

Received: January 7, 2023

Scheme 1. Synthesis of the Gold(I) Complexes 1 and 2 (A) and Their Heterometallic Cu(I)/Au(I) Derivatives (B, C)

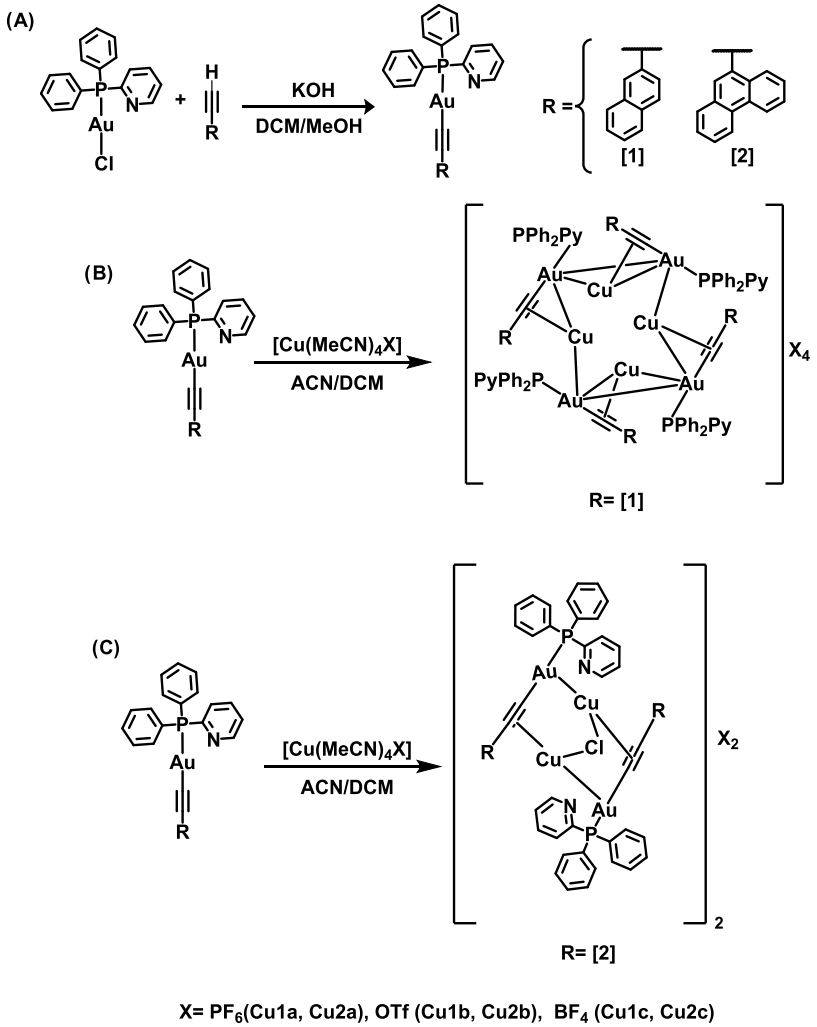

X= PF_6(Cu1a, Cu2a), OTf (Cu1b, Cu2b), BF_4 (Cu1c, Cu2c)

by heterometallic interactions with the different metals in the cluster core.[37,38] Population of the T_1 triplet excited state is quite common in this type of complexes containing heavy atoms that are responsible for the resulting phosphorescence emission.

Compounds with populated triplet excited states can also be involved in singlet oxygen ($^1O_2$) production. This research area is attracting increasing attention over recent years since it plays a key role in a diverse array of processes such as wastewater treatment, blood sterilization, photocatalytic processes, and photodynamic therapy.[39] As photosensitizers, many organic compounds were studied to produce singlet oxygen with high quantum yields (QY). Usually, these compounds are nanotubes,[40] graphene derivatives,[41] and diverse molecules with π-donors and π-acceptors in their structure to promote the charge transfer to the triplet state.[42−45] In comparison with the organic compounds, photosensitizers containing metal atoms used as $^1O_2$ sensitizers are less studied and are mainly focused on metalloporphyrin, metal−organic framework (MOF), and nanoparticles.[46−48]

To the best of our knowledge, there are very few reports in the literature regarding organometallic gold(I) complexes used as photosensitizers with yields from low−moderate to high (20−57%).[32,49−54] Additionally, to the best of our knowledge, no Au(I)/Cu(I) heterometallic clusters have yet been explored in this field. We are convinced that they deserve to be analyzed in this field in order to find out if the increase of the heavy atom effect and the cooperative effect of two different metals can positively affect the resulting energy transfer with oxygen.

Taking all of this into consideration, in this work, we have synthesized two gold(I) complexes containing a P−N polydentate ligand and a polyaromatic chromophore (naphthalene or phenanthrene) coordinated to the metal atom through an alkynyl group. These compounds have been used as precursors to obtain heterometallic clusters by the coordination of Cu(I) in the chemical structure. As is known, both the N-atom in the phosphane ligand and the alkynyl moiety may coordinate with the copper(I) metal centers and provide ancillary support to bimetallic cluster formation, thanks to the additional expected coordination to the Au(I) atoms (Au(I)···Cu(I) weak contacts).[34,35,55−57] The obtained heterometallic complexes have been studied as red phosphorescence emitters and singlet oxygen photosensitizers.

RESULTS AND DISCUSSION

Synthesis and Characterization. The synthesis of the gold(I) complexes **1** and **2** has been carried out following a similar procedure previously used in our research group (Scheme 1A),[58−60] that is, the deprotonation of the terminal

https://doi.org/10.1021/acs.inorgchem.3c00046
Inorg. Chem. XXXX, XXX, XXX−XXX

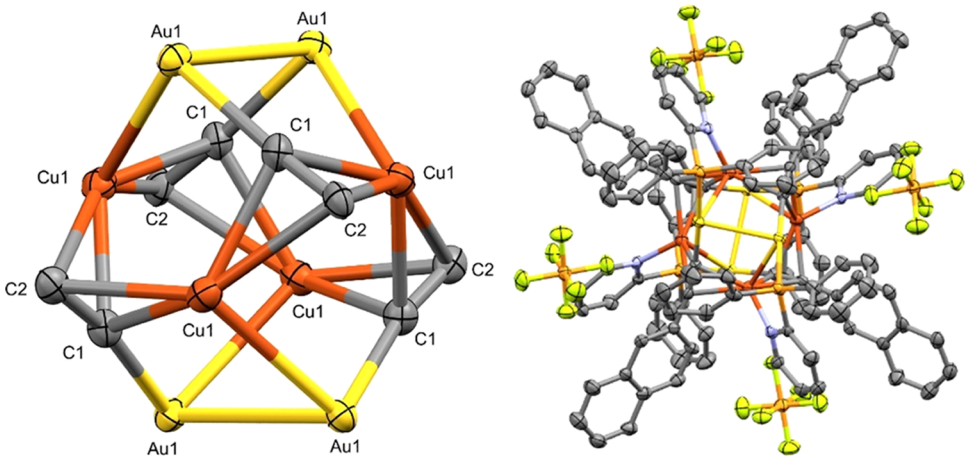

Figure 1. Left: cluster core on **Cu1a** on the axis *c*. Right: structure of complex **Cu1a** on the axis *b*. Atom colors: yellow, gold; bronze, copper; orange, phosphorus; light green, fluorine (thermal parameters at a 50% probability; hydrogen atoms have been omitted for clarity).

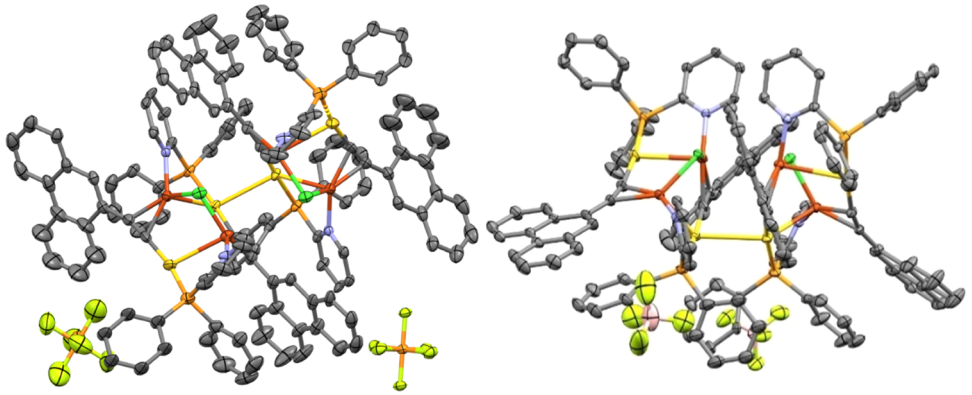

Figure 2. Structure of the cluster core of complexes **Cu2a** (left) and **Cu2c** (right) on the axis *c*. (Atom colors: yellow = gold, bronze = copper, orange = phosphorus, light green = fluorine, green = chlorine, pink = boron; thermal ellipsoids at a 50% probability; hydrogen atoms and solvate molecules have been omitted for clarity).

alkynyl moiety and the subsequent reaction with the previously synthesized $Au(pyPPh_2)Cl$[61] compound.

Compounds **1** and **2** were reacted stoichiometrically with different copper(I) salts (PF_6: **a**; OTf: **b**; BF_4: **c**) in dichloromethane yielding six new heterometallic Au(I)−Cu(I) complexes (Scheme 1B). The compounds were obtained in pure forms after recrystallization with dichloromethane/hexane. Different heterometallic structures were obtained depending on the chromophore. In the case of the naphthalene derivatives, the resulting cluster consists of a symmetrical structure with a Au_4Cu_4 core (Scheme 1B), while a more open structure is generated in the case of the phenanthrene compounds that include chlorine bridging atoms connecting the Cu metal centers in the crystallization process (Scheme 1C). White powders were obtained for the gold(I) compounds, while orange-red solids were obtained for the heterometallic ones, all of them with moderate−high yields.

The ^1H, ^{19}F, and ^{31}P NMR and IR spectroscopies together with electrospray ionization mass spectrometry (ESI-MS) (+) and (−) mass spectrometry demonstrate in all cases the correct formation of the desired compounds. The ^1H NMR spectra of **1** and **2** (see Figures S1 and S3, respectively, in the Supporting Information (SI)) display the disappearance of the signal at 3.18 and 3.48 ppm, respectively, which corresponds to the terminal alkynyl protons and indicates the coordination of the gold(I) atom. The $[M + H]^+$ peaks recorded in both cases in the corresponding ESI-MS(+) spectra verify the correct formation of the desired products (Figures S5 and S6 in the SI).

The ^1H NMR spectra display that the protons in the ortho position to the nitrogen atom in the pyridyl ring of phosphane are affected by the coordination of the Cu(I) center in the case of **1a−c**, mainly for **Cu1a** and **Cu1b** with a 0.3−0.5 ppm downfield shift in comparison with **1** (Figure S31).[19] This effect is even more pronounced for the series of complexes **2** and **Cu2a−Cu2c**, with a 0.5−0.6 ppm downfield shift of this proton (Figure S32). We can also observe that both naphthalene and phenanthrene protons become broader and upfield-shifted upon copper(I) coordination, probably due to the repolarization of the bond product of SOC influenced for the cluster formation[62,63] or the rigidity of the molecule as a result of cluster formation.[55] In fact, the Cu(I) cation can be bonded both to the pyridine moiety and through the alkynyl group. These interactions may exist with both intermolecular and intramolecular characters. Indeed, the first evidence of the presence of this kind of interaction in the solid state was given by the IR spectra of the compounds. It was observed that the $\nu(C{\equiv}C)$ vibration of **1** and **2** (observed at 2111 and 2112 cm^{-1}, respectively) was shifted to 2005−2077 cm^{-1} indicating a slight decrease in the bond order by the weak coordination to the second metal center.

https://doi.org/10.1021/acs.inorgchem.3c00046
Inorg. Chem. XXXX, XXX, XXX−XXX

Table 1. Main Distances and Angles of Complexes Cu1a, Cu2a, and Cu2c

	distances (Å)					angles (deg)		
complex	Au1−Au1	Au1−Cu1	Cu1−N22	Cu1−C2	Au2−Au2	C1−Au1−P1	C1−Cu1−Au1	N22−Cu1−Au1
Cu1a	2.9875(7)	2.7197(9)	2.062(6)	2.167(5)	2.9700(7)	176.4(2)	88.2(2)	93.1(2)
Cu2a	3.0187(6)	2.790(1)	2.007(6)	2.033(7)		176.7(2)	97.0(2)	89.5(2)
Cu2c	2.9940(5)	2.810(1)	2.026(5)	2.079(7)		171.9(2)	105.5(2)	93.3(1)

Table 2. Photophysical Properties of Compounds 1 and 2 and Their Au(I)/Cu(I) Heterometallic Complexes in Solution[a]

complex	λ_{max} Abs, nm ($\varepsilon \times 10^3$ cm^{-1} m^{-1})	λ_{max} Em (nm)	Φ_{fl} (air-eq/N_2 sat)	Φ_{phos} (air-eq/N_2 sat)	τ (air-eq/N_2 sat, μs)
1	315 (23.6)	356, 505, 545	0.002/0.003	0.001/0.019	0.004/0.005
2	315 (22.5)	384, 535, 579	0.004/0.005	0.002/0.014	0.005/0.006
Cu1a	315 (20.2), 333 (16.4), 355 (9.1)	642		0.02/0.05	0.28/0.29
Cu1b	315 (11.3), 333 (10.3), 355 (6.0)	643		0.02/0.06	0.32/0.34
Cu1c	315 (11.9), 333 (10.2), 355 (9.0)	643		0.01/0.02	0.10/0.12
Cu2a	315 (17.6),333 (20.9), 355 (19.9)	628		0.06/0.13	4.8/7.5
Cu2b	315 (21.2), 333 (24.8), 355 (23.3)	630		0.06/0.12	4.2/6.7
Cu2c	315 (11.8), 333 (12.9), 355 (11.0)	629		0.05/0.09	4.3/6.9

[a] Φ_{Fl} = fluorescence QY; Φ_{Phos} = phosphorescence QY. τ = lifetimes.

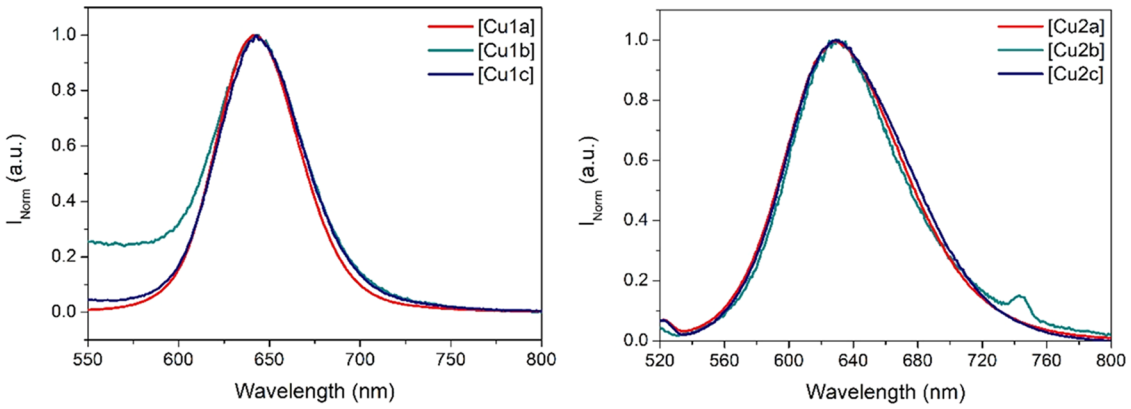

Figure 3. Normalized emission spectra of complexes **Cu1a−Cu1c** (left) and **Cu2a−Cu2c** (right) in 10^{-5} M CH_2Cl_2 solutions (λ_{exc} = 450 nm).

The heterometallic Au(I)/Cu(I) complexes present better solubility in common organic solvents and permit the growth, in some cases, of single crystals suitable for X-ray diffraction to determine the structure and coordination motifs of the products. Single crystals of **Cu1a** were grown by slow evaporation of a dichloromethane solution of the compound. The structure of **Cu1a** shows a cluster core containing four Au(I) metal centers and four Cu(I) metal centers in the unit $[AuCu(PyPPh_2)(C{\equiv}CC_{10}H_7)]_4$ with two different distances of the Cu(I) to the centroid generated by the two C≡C moieties ($d_{Cu-C{\equiv}C(centroid)}$ = 2.099(5) and 2.153(5) Å) and a Cu···Cu distance of 3.297 Å. The angles around the Cu centers correspond to N−Cu−centroid(C≡C) of 102.1(2)° and Au−Cu−centroid(C≡C) of 95.0(2)°. For the Au(I) centers, the d_{Au-P} = 2.286(2) Å, d_{Au-C} = 2.029(6) Å, the angle P−Au−C = 176.4(2)°, P−Au−Cu = 82.40(5)°, and C−Au−Cu = 97.8(2)°. The Au(I)−Cu(I) heterometallic interaction in the cluster presents a d_{Au-Cu} = 2.7197(9) Å (Figure 1).

The crystal packing of the compound presents the individual clusters producing empty inner cavities that are occupied by the PF_6^- counterion (Figure S33).

Red crystals of **Cu2a** and **Cu2c** were grown by the evaporation of the sample in chloroform, and the corresponding cluster core structures are presented in Figure 2. The asymmetric unit cell of **Cu2a** shows a cluster structure with two counteranions. We observe that, in both cases, these clusters derived from phenanthrene present a more open conformation in comparison with the analogous naphthalene **Cu1a**, which could be ascribed to the higher volume of the chromophore and to the inclusion of two chlorine atoms (that may come from the formation of some HCl traces from the solvent of crystallization during the crystal growth) bonded to the Cu(I) atoms. As observed for **Cu2a**, this compound presents two different distances to the centroid generated by the two C≡C moieties with a $d_{Cu-C{\equiv}C(centroid)}$ = 2.036(6) and 2.042(6) Å (2.053(7) and 2.013(7) Å, respectively, for **Cu2c**), which are shorter than in the naphthalene analogous and a Cu···Cu distance of 3.543 Å. The angles for N−Cu−centroids(C≡C) of **Cu2a** are between 127.98(3)−132.44(3)°, which are similar to the **Cu2c** complex with 126.46(2)−133.83(2)° for equivalent atom connectivity; this is caused by the inclusion of chlorine atoms in the metallic clusters that open the metallic shell being the angles Cu−Cl−Cu = 95.55(7)° (101.51(7)° for **Cu2c**), Au−Cu−centroid-(C≡C) = 101.5(2)° (105.5(2)° for **Cu2c**) and Cl−Cu−centroid(C≡C) = 140.3(2)° (142.1(2)° for **Cu2c**). The main parameters around the Au(I) centers are d_{Au-P} = 2.280(2) and 2.253(2) Å, d_{Au-C} = 2.012(6) and 2.011(7) Å, and the angles P−Au−C = 176.7(2) and 171.1(2)°, P−Au−Cu = 80.71(5) and 81.35(5)° and C−Au−Cu = 97.0(2) and 99.8(2)° for

https://doi.org/10.1021/acs.inorgchem.3c00046
Inorg. Chem. XXXX, XXX, XXX−XXX

Table 3. Radiative (k_r) and Nonradiative (k_{nr}) Constants of the Gold(I) Complexes 1 and 2 and Their Heterometallic Au(I)−Cu(I) Complexes in Solution Considering the Phosphorescence Emission

complex	k_r (air-eq) × 10^5 s^{-1}	k_{nr} (air-eq) × 10^5 s^{-1}	k_r ($N_{2\ sat}$) × 10^5 s^{-1}	k_{nr} ($N_{2\ sat}$) × 10^5 s^{-1}
1			40	1960
2			16.7	1680
Cu1a	0.7	34.5	1.8	33.6
Cu1b	0.6	31.1	1.8	27.5
Cu1c	1.0	102	1.7	81.7
Cu2a	0.1	2.0	0.1	1.2
Cu2b	0.1	2.2	0.2	1.3
Cu2c	0.1	2.2	0.2	1.3

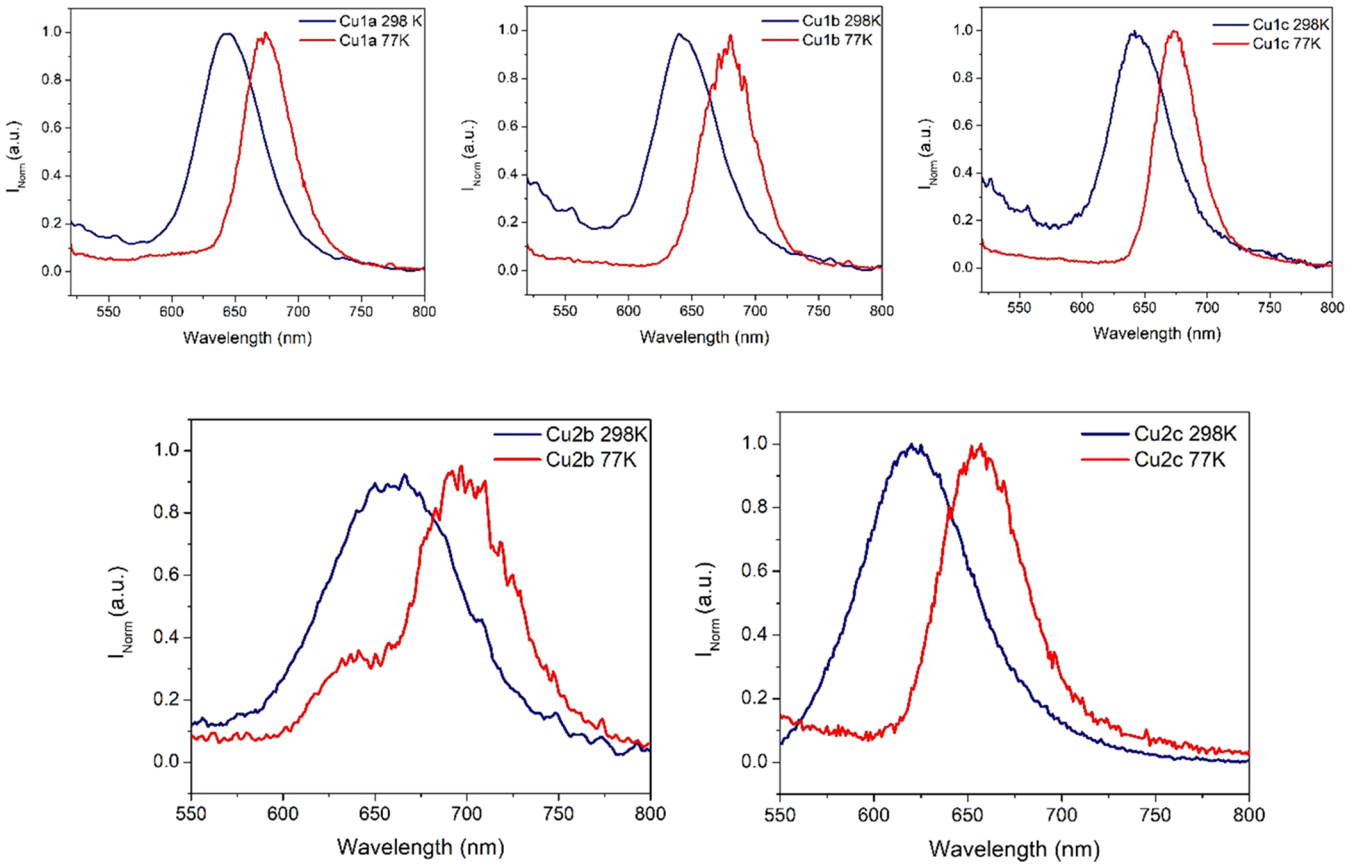

Figure 4. Normalized emission spectra of complexes **Cu1a−Cu1c** (above) and **Cu2b−Cu2c** (below) in the solid state at 298 and 77 K (λ_{exc} = 450 and 470 nm, respectively).

Cu2a and **Cu2c**, respectively. The Au(I)/Cu(I) heterometallic interactions present a distance d_{Au-Cu} = 2.828(1) and 2.810(1) Å for **Cu2a** and **Cu2c**, slightly larger than in the naphthalene analogous, probably due to the resulting more open structure (Table 1).

Photophysical Properties. The absorption and emission spectra of the heterometallic complexes and their respective gold(I) precursors were measured in 10^{-5} M CH_2Cl_2 solutions at room temperature (Table 2 and Figures S34−S43). The absorption spectra of the compounds show vibronically structured bands at 315 and 333 nm for **1** and **2**, respectively, that are assigned to $\pi-\pi^*$ intraligand transitions.[64] A new band centered at 355 nm appears for the heterometallic cluster complexes **Cu1a−Cu1c** and **Cu2a−Cu2c**. This band becomes broader and red-shifted in these complexes due to the presence of metallophilic interactions and the resulting cluster-centered (^{3}CC) transitions (Figures S38−S43).[65]

Fluorescence emission has been recorded for the gold(I) complexes in solution at room temperature with emission maxima at 356 and 384 nm for **1** and **2**, respectively. Dual emission has been recorded when the samples are deoxygenated with a phosphorescence band at 545 for **1** and 535 nm for **2** (Figures S38−S43). The vibronical resolution of both fluorescence and phosphorescence bands allows us to assign these transitions to metal-perturbed IL emissions (^{1}IL and ^{3}IL) located at the ethynylnapthalene or ethynylphenanthrene units. Phosphorescence emission is much more favored in the case of the naphthalene compounds.

Interestingly, pure room-temperature phosphorescence has been observed for all heterometallic complexes with broad bands centered at *ca.* 642 nm for **Cu1a−Cu1c** and at *ca.* 630 nm for **Cu2a−Cu2c** (Figures 3, S38, and S41). This emission appears in air-equilibrated solutions and is not affected by the nature of the counteranion. The resulting emission is red-

https://doi.org/10.1021/acs.inorgchem.3c00046
Inorg. Chem. XXXX, XXX, XXX−XXX

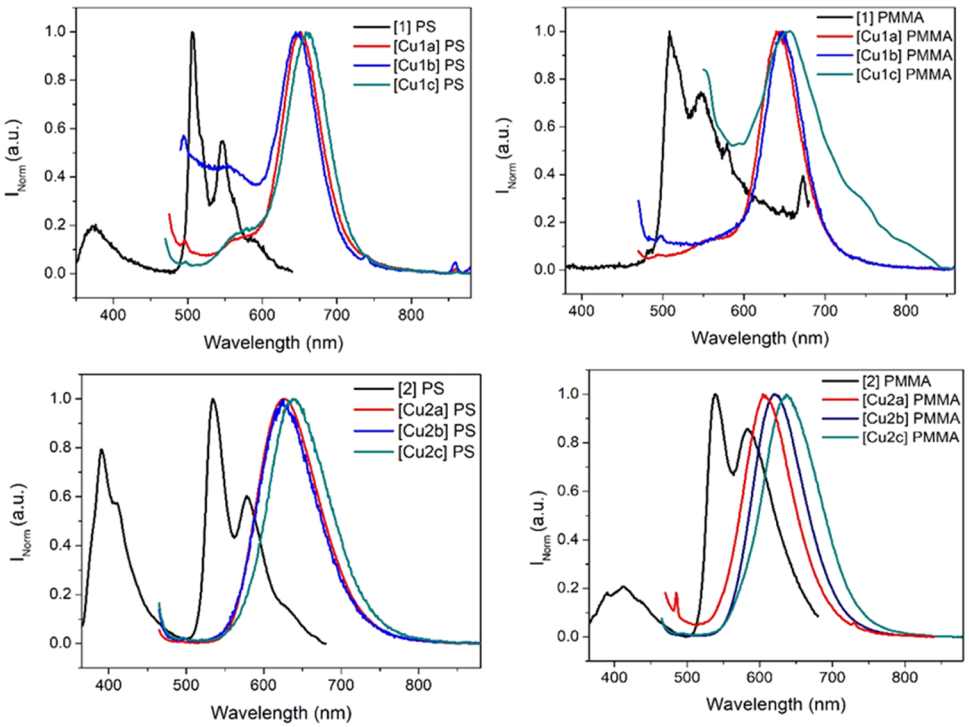

Figure 5. Cu1a−c (top) and **Cu2a−c** (bottom) complexes supported in polymeric solid matrices PS (left) and PMMA (right). λ_{exc} = 450 nm.

shifted with respect to the gold(I) homometallic compounds as previously observed with other Au/Cu heterometallic systems containing the same pyPPh$_2$ phosphane previously reported in the literature. These transitions have been ascribed to an admixture of IL/LL′/LAuMCT transitions.[37,55,56,66−70] In particular, the ligand-to-metal charge-transfer character of the transitions has been previously attributed thanks to time-dependent density-functional theory (TDDFT) calculations, and this charge-transfer process is observed to increase in the heterometallic compounds with respect to the homometallic, with the main role of the copper center.[55,56] This would correlate with the observed resulting emission red shift.

Thus, we do not expect any type of interaction in solution between the metallic core and the counterions.[71] The different properties between the gold(I) parent compounds and the heterometallic compounds support the successful formation and stability of the new Au(I)/Cu(I) heterometallic structures in solution. Unfortunately, we did not manage to detect the desired Au_4Cu_4 full core in the mass spectra. Nevertheless, the resulting room-temperature phosphorescence recorded for **Cu1a−Cu1c** and **Cu2a−Cu2c** strongly supports the formation of the new heterometallic systems, with completely different emission profiles with respect to their parent gold(I) homometallic complexes and, thus, the presence of new (heterometallic) structures in solution.

The recorded photoluminescence quantum yields (QY)s are larger for the phenanthrene heterometallic clusters with respect to the analogous containing naphthalene. In both cases, the triflate and hexafluorophosphate derivatives (**a** and **b** compounds) display QY values larger than the tetrafluoroborate compounds **c** in both air-equilibrated and N_2-saturated solutions, with larger values (approximately double) in the absence of oxygen (Table 2). Lifetime measurements are around 0.1−0.3 μs for **Cu1a−Cu1c** and 5−8 μs for **Cu2a−Cu2c**; the heterometallic complexes are slightly affected by the presence of oxygen, being 2 orders of magnitude larger than the corresponding values measured for the gold(I) complexes that display a lifetime of nanoseconds.

The radiative (k_r) and nonradiative constants (k_{nr}) were calculated in all cases, and we can observe first that the very large k_{nr} values of compounds **1** and **2** are responsible for the lack of phosphorescence emission in air-equilibrated solutions and very weak in N_2-saturated samples. On the other hand, again, the counterion is affecting only series **1** and not series **2** in both air-equilibrated and N_2-saturated solutions. The nonradiative contributions are also more important in series **1** in agreement with their lower recorded quantum yields (Table 3).

The emissions in the solid state for the six cluster complexes **Cu1a−Cu1c** and **Cu2a−Cu2c** were measured at 298 and 77 K (Table S1 in the SI and Figure 4). A red shift of the emission is recorded in almost all cases (except for **Cu2a**) when the powders are cooled (Figure 4). The observed red shift at low temperatures has been observed in other heterometallic Au(I)/Cu(I) complexes reported in the literature.[72−74]

The emission of all of the compounds has also been analyzed when the samples are immobilized within two different polymeric matrices (polystyrene, PS, and poly(methyl methacrylate), PMMA) using a low amount of the compounds (1%) as doping agents. Interestingly, and as a difference with what was previously observed in solution, room-temperature phosphorescence has been recorded as the main emission also for the gold(I) complexes **1** and **2**. The vibronically structured band allowed us to assign this phosphorescence to a metal-perturbed ^{3}IL transition. As expected for a more rigid environment, the recorded QY in this media are larger than those previously recorded in solution (see Table 5).

The heterometallic compounds do not display the same behavior in both series of complexes. **Cu1a−c** heterometallic compounds present a broad phosphorescence band at *ca.* 650 nm in both PS and PMMA (Figure 5). This band is closer to the one recorded in the solid state at 77 K.

https://doi.org/10.1021/acs.inorgchem.3c00046
Inorg. Chem. XXXX, XXX, XXX−XXX

Table 4. Quantum Yield (QY) Values (Φ) and Emission Lifetimes (τ) of Gold(I) Complexes 1 and 2 and Their Heterometallic Au(I)−Cu(I) Complexes in Solid State and Supported in Polymeric Matrices[a]

complex	$\Phi_{Fl/Phos}$ (solid state)	$\Phi_{Fl/Phos}$ (PMMA)	$\Phi_{Fl/Phos}$ (PS)	$\tau_{Fl/Phos}$ (μs) solid state	$\tau_{Fl/Phos}$ (μs) PMMA	$\tau_{Fl/Phos}$ (μs) PS
1		0.002/0.046	0.002/0.010		1.1×10^{-3}/0.166	7.2×10^{-3}/0.006
2		0.006/0.030	0.009/0.010		2.2×10^{-3}/0.056	6.1×10^{-3}/0.012
Cu1a	−/0.04	−/0.04	−/0.01	−/2.15	−/0.137	−/0.093
Cu1b	−/0.01	−/0.03	−/0.01	−/0.05	−/0.121	−/0.089
Cu1c	−/0.01	−/0.02	−/0.01	−/1.15	−/0.071	−/0.056
Cu2a	−/0.11	−/0.15	−/0.08	−/1.65	−/14.65	−/5.00
Cu2b	−/0.07	−/0.09	−/0.05	−/1.04	−/15.34	−/7.38
Cu2c	−/0.05	−/0.08	−/0.03	−/0.77	−/15.36	−/5.98

[a] Φ_{Fl} = fluorescence QY; Φ_{Phos} = phosphorescence QY.

On the other hand, the **Cu2a−c** compounds are more affected by the polymer, mainly in PMMA where a red shift of *ca.* 100 nm is observed in the order PF_6^- < OTf^- < BF_4^- (Figure 5). This can be rationalized by the fact that the less bulky counterion BF_4^- can be more dispersed within the polymer, allowing larger interactions and dispersion of the heterometallic cluster in the matrix than in the case of larger counterions. On the contrary, there is no significant shift in the emission of the samples when they are immobilized in the more apolar PS polymer. All compounds present an enhancement of phosphorescence QY in PMMA in comparison with the PS matrix, in agreement with recent studies with alkynyl gold(I) complexes supported in these matrices (Table 4).[20,75]

Singlet Oxygen Production. The use of the two gold(I) complexes **1** and **2** and the six Au(I)−Cu(I) clusters as $^1O_2$ photosensitizers has been tested since we wondered if the presence of such many heavy atoms in close proximity may have a direct influence on the population of the triplet excited state and the energy-transfer process to $^3O_2$. These studies have been carried out by the direct measure of the characteristic $^1O_2$ emission at 1270 nm, which corresponds to $^1\Delta_g \rightarrow {}^3\sum_g^-$ transition upon excitation of the samples at λ_{exc} = 365−380 nm in air-equilibrated acetonitrile solutions and using perinaphthenone as the reference (Φ_Δ = 79%).

The results show that all phenanthrene derivatives behave slightly better as $^1O_2$ photosensitizers than the analogous naphthalene derivatives (Table 5 and Figures S56−S63) with $\Phi_\Delta \sim 50$ for series **2** and ∼40% for series **1**. The two BF_4^- derivatives (**Cu1c** and **Cu2c**) display values slightly lower than the other complexes.

Recent studies with alkynyl gold(I) derivatives show $^1O_2$ production in the range of 9−29%.[53,54] Thus, we managed to improve the singlet oxygen quantum yield values with our compounds although the expected heterometallic metallophilic interactions do not seem to positively affect the photosensitizing behavior, possibly due to the interference of the counterion (mainly the smaller BF_4^-) with the intermolecular contacts in solution or due to the different energy levels between the heterometallic and homometallic systems.

Table 5. $^1O_2$ Quantum Yield (Φ_Δ) Calculated for All Compounds in Acetonitrile Air-Equilibrated Solutions

compound	Φ_Δ (%)
1	40
Cu1a	36
Cu1b	37
Cu1c	25
2	50
Cu2a	42
Cu2b	47
Cu2c	38

CONCLUSIONS

The addition of Cu(I) salts to gold(I) complexes containing alkynylnaphthalene and alkynylphenanthrene as chromophores allowed us to obtain heterometallic cluster complexes with different emissive properties that differ mainly on the bulkiness of the chromophore. The spectra in the solution of clusters induce a red shift and a pure room phosphorescence emission in air-equilibrated samples in comparison with the Au(I) analogous complexes that only display phosphorescence in the absence of oxygen. The phosphorescence of the gold(I) compounds can also be induced when they are introduced as doping agents of polymeric organic matrices (PMMA and PS). The interaction with the matrix has a larger effect on the phenanthrene heterometallic compounds in PMMA. All compounds present denotable values of singlet oxygen quantum yields in comparison with the literature, offering a platform to improve the research on the use of organometallic complexes as singlet oxygen photosensitizers.

The formation of heterometallic clusters had a direct influence on the resulting phosphorescence and red emissions, though only a minimal effect was seen on the interaction with $^3O_2$ toward their use as photosensitizers.

EXPERIMENTAL SECTION

All air- and moisture-sensitive manipulations were carried out with standard Schlenk techniques under a nitrogen atmosphere. Solvents were purchased from commercial sources and dried by distillation under a nitrogen atmosphere. Reagents 2-ethynyl naphthalene, 9-ethynylphenanthrene, KOH, 2-(diphenylphosphino)pyridine ($PyPh_2P$), $[Cu(MeCN)_4]PF_6$, $[Cu(MeCN)_4]OTf$, and $[Cu(MeCN)_4]BF_4$ were purchased from commercial sources and used without further purification. [Au(tht)Cl],[76] the phosphanegold(I) chloride precursor [$PyPh_2PAuCl$],[61] was prepared from the reaction of [Au(tht)Cl] with the phosphane $PyPh_2P$.

Infrared spectra have been recorded on an FT-IR 520 Nicolet spectrophotometer. ^1H NMR (δ(TMS) = 0.0 ppm) and ^{31}P NMR (δ(85% H_3PO_4) = 0.0 ppm) spectra have been obtained on Bruker 400 and Bruker 500 (Universitat de Barcelona) instruments. Electrospray mass spectra (+) have been recorded on a Fisons VG Quatro spectrometer (Universitat de Barcelona). Absorption spectra were obtained in a 5 or 10 mm quartz cuvette in acetonitrile on a Varian Cary 100 Bio UV spectrophotometer. The emission spectra of the compounds in solution were obtained in a fluorescence quartz cuvette of 10 mm path length, using a Horiba-Jobin-Yvon SPEX Nanolog spectrofluorimeter, using slits of 2 nm. Low-temperature measurements were recorded using a Dewar adapted to the sample

https://doi.org/10.1021/acs.inorgchem.3c00046
Inorg. Chem. XXXX, XXX, XXX−XXX

location of the spectrofluorometer. Quantum yields have been recorded on a Hamamatsu absolute PL quantum yield spectrometer C11347 upon excitation of the samples at 330 nm. Luminescence lifetimes were measured on a JYF-DELTAPRO-NL equipment upon excitation of the samples with a 390 nm NanoLED and collecting the decays through a bandpass filter of 550, 600, or 650 nm, depending on the emission maximum. The best fittings correspond to biexponential decays, and the indicated values correspond to the average considering the respective amplitudes.

The single-crystal X-ray data for **Cu1a** and **Cu2a** were collected at 120 K using an Agilent SuperNova diffractometer with an Eos detector using mirror-monochromated Mo Kα (λ = 0.71073 Å) radiation. The single-crystal X-ray data for **Cu2c** were collected at 120 K using an Agilent SuperNova dual wavelength diffractometer with an Atlas detector using mirror-monochromated Cu Kα (λ = 1.54184 Å) radiation. All structures were solved by intrinsic phasing (SHELXT)[77] and refined by full-matrix least squares on F^2 using Olex2,[78] utilizing the SHELXL module.[79] Anisotropic displacement parameters were assigned to non-H atoms, and isotropic displacement parameters for all H atoms were constrained to multiples of the equivalent displacement parameters of their parent atoms with $U_{iso}(H)$ = 1.2 U_{eq} of their respective parent atoms. The X-ray single-crystal data and CCDC numbers of all new structures are included in the Supporting Information.

Spectroscopic Measurements. All measures were realized using spectroscopic quality solvents in 10^{-5} M concentration. For $^1O_2$ measurements, the dichloromethane solutions were adjusted to an A = 1 in the peak of excitation wavelengths.

Singlet Oxygen Quantum Yields. Room-temperature singlet oxygen emission was detected at 1270 nm with a Horiba-Jobin-Yvon SPEX Nanolog spectrofluorimeter (Universitat de Barcelona) using the DSS-IGA020L detector. The use of a Schott RG 1000 filter was essential to eliminate from the infrared signal all of the first harmonic contribution of sensitizer emission in the region below 850 nm. The singlet oxygen formation quantum yield was then determined by the direct measurement of the phosphorescence at 1270 nm following irradiation of the aerated solution in dichloromethane of the samples. Perinaphthenone in dichloromethane was used as a standard reference, applying eq 1

$$\Phi_\Delta = \frac{\frac{I_{sample}}{A_{sample}}}{\frac{I_{ref}}{A_{ref}}} \times 79\% \quad (1)$$

Synthesis and Characterization. *[(PyPh$_2$P)AuC≡CNaph] (**1**).* KOH (17 mg, 0.303 mmol, 1.5 equiv) was added to a methanol (5 mL) solution under a N_2 atmosphere. 2-Ethynyl-naphthalene (30.7 mg, 0.202 mmol, 1 equiv) was added. The mixture was stirred for 2 h at 25 °C. Then, a solution of [(PyPh$_2$P)AuCl] (100 mg, 0.202 mmol, 1 equiv) in 3 mL of dichloromethane was slowly added. After 76 h, the solvents were removed under a vacuum. The solid was dissolved in 1 mL of dichloromethane and precipitated with 3 mL of hexane. **1** was obtained as a white solid (102 mg, 82%). ^{1}H NMR: (dimethyl sulfoxide (DMSO)-d_6 400 MHz) δ = 8.85 (d, J = 4.7 Hz, 1H), 8.04−7.97 (m, 1H), 7.84 (ddd, J = 15.5, 12.1, 6.6 Hz, 4H), 7.77−7.71 (m, 1H), 7.69−7.57 (m, 10H), 7.53−7.45 (m, 2H), 7.42 (dd, J = 8.5, 1.6 Hz, 1H), 7.34 (dd, J = 8.5, 1.6 Hz, 1H) ppm; ^{31}P NMR: (DMSO-d_6 162 MHz) δ = 41.29 ppm. ESI (m/z): 1071.15 [2M-Naph]$^+$, 723.13 [Au(PyPhos)$_2$]$^+$, 612.11 [M + H]$^+$, IR (cm^{-1}): ν = 3039.50 (ar), 2111.25 (C≡C), 1590.85 (C═N), 1480.63 (C−H ar), 1100.98 (P−C).

*[(PyPh$_2$P)$_4$Cu$_4$Au$_4$(C≡CNaph)$_4$][PF$_6$]$_4$ (**Cu1a**).* In a sealed flask under a N_2 atmosphere, **complex 1** (10 mg, 0.0178 mmol, 1 equiv) was added in 3 mL of CH_2Cl_2 in stirring for 5 min. Then, [Cu(MeCN)$_4$]PF$_6$ (6.09 mg, 0.0178 mmol, 1 equiv) dissolved in 2 mL of CH_2Cl_2 was added. After 3 h, the solution was reduced to dry under vacuum. The solid was dissolved in 1 mL of dichloromethane and precipitated with 2 mL of hexane. **Cu1a** was obtained as a red-orange solid (9.2 mg, 67%). ^{1}H NMR: ($CDCl_3$, 400 MHz) δ = 8.79 (d, J = 4.8 Hz, 1H), 8.00 (dd, J = 14.9, 7.4 Hz, 2H), 7.86−7.77 (m, 1H), 7.74−7.65 (m, 6H), 7.57−7.43 (m, 9H), 7.43−7.37 (m, 3H) ppm; ^{19}F NMR: ($CDCl_3$ 162 MHz) δ = −71.35 ppm (d, J_{P-F} 714.9 Hz, 6F), ^{31}P NMR: ($CDCl_3$ 162 MHz) δ = 33.6 (s), −141.5 (hept) ppm. ESI (m/z): 1897.25 [3M + Cu + H]$^+$, 1383.04 [2M + 2Cu + Cl + H]$^+$, 1285.14 [2M + Cu + H]$^+$, 723 [Au(PyPhos)$_2$]$^+$, IR (cm^{-1}): ν = 2962.34 (ar), 2012.93 (C≡C), 1584.88 (C═N), 1098.50 (P−C), 835.68 (P−F).

*[(PyPh$_2$P)$_4$Cu$_4$Au$_4$(C≡CNaph)$_4$][OTf]$_4$ (**Cu1b**).* In a sealed flask under an N_2 atmosphere **complex 1** (10 mg, 0.0178 mmol, 1 equiv) was added in 3 mL of CH_2Cl_2 under stirring for 5 min. Then, [Cu(MeCN)$_4$]OTf (6.16 mg, 0.0178 mmol, 1 equiv) dissolved in 2 mL of CH_2Cl_2 was added. After 3 h, the solution was reduced to dryness under vacuum. The solid was dissolved in 1 mL of dichloromethane and precipitated with 2 mL of hexane. **Cu1b** was obtained as an orange solid (10.2 mg, 85%). ^{1}H NMR: ($CDCl_3$, 400 MHz) δ = δ 8.79 (s, 1H), 8.03 (s, 1H), 7.80 (dd, J = 8.6, 5.4 Hz, 2H), 7.69 (dd, J = 13.5, 7.4 Hz, 4H), 7.57−7.32 (m, 13H) ppm; ^{19}F NMR: ($CDCl_3$ 162 MHz) δ = −78.12 ppm (s, 3F), ^{31}P NMR: ($CDCl_3$ 162 MHz) δ = 42.4 (s) ppm. ESI (m/z): 1896.24 [3M + Cu + H]$^+$, 1383.04 [2M + 2Cu + Cl + H]$^+$, 1285.14 [2M + Cu + H]$^+$, 1071.15 [2M + H]$^+$, 723.13 [Au(PyPhos)$_2$]$^+$, IR (cm^{-1}): ν = 2961.91 (ar), 2042.32 (C≡C), 1585.12 (C═N), 1458.15 (C−H), 1258.00 (B−F), (P−C),1093.55 (P−C).

*[(PyPh$_2$P)$_4$Cu$_4$Au$_4$(C≡CNaph)$_4$][BF$_4$]$_4$ (**Cu1c**).* In a sealed flask under a N_2 atmosphere, complex 1 (10 mg, 0.0178 mmol, 1 equiv) was added to 3 mL of CH_2Cl_2 under stirring for 5 min. Then, [Cu(MeCN)$_4$]BF$_4$ (5.12 mg, 0.0178 mmol, 1 equiv) dissolved in 2 mL of CH_2Cl_2 was added. After 3 h, the solution was reduced to dryness under vacuum. The solid was dissolved in 1 mL of dichloromethane and precipitated with 2 mL of hexane. **Cu1c** was obtained as a red-orange solid (9.1 mg, 78%). ^{1}H NMR: ($CDCl_3$, 400 MHz) δ = 8.80 (s, 1H), 8.0 (m, 2H), 7.86−7.76 (m, 3H), 7.70 (dd, J = 13.3, 7.5 Hz, 5H), 7.52 (d, J = 7.5 Hz, 2H), 7.47 (d, J = 6.1 Hz, 3H), 7.44−7.34 (m, 2H) ppm; ^{19}F NMR: ($CDCl_3$ 162 MHz) δ = −150.29 ppm (s, 4F), ^{31}P NMR: ($CDCl_3$ 162 MHz) δ = 32.27 (s) ppm. ESI (m/z): 1346.93 [2M + 2Cu + H]$^+$, 1071.10 [2M + H]$^+$, 723.13 [Au(PyPhos)$_2$]$^+$, IR (cm^{-1}): ν = 2962.08 (ar), 2024.47 (C≡C), 1586.24 (C═N), 1098.19 (P−C), 1054.06 (B−F).

*[(PyPh$_2$P)AuC≡CPhen] (**2**).* KOH (17 mg, 0.303 mmol, 1.5 equiv) was added to a methanol (5 mL) solution under a N_2 atmosphere. 9-Ethynylphenanthrene (40.8 mg, 0.202 mmol, 1 equiv) was added. The mixture was stirred for 2 h at 25 °C. Then, a solution of [(PyPh$_2$P)AuCl] (100 mg, 0.202 mmol, 1 equiv) in 3 mL of dichloromethane was slowly added. After 24 h, the solvents were removed under vacuum. The solid was dissolved in 1 mL of dichloromethane and precipitated with 3 mL of hexane. **2** was obtained as a white solid (52 mg, 46%). ^{1}H NMR: (DMSO-d_6 400 MHz) δ = 8.90−8.72 (m, 3H), 8.67−8.54 (m, 1H), 8.07−7.89 (m, 3H), 7.84−7.54 (m, 16H) ppm; ^{31}P NMR: (DMSO-d_6 162 MHz) δ = 40.41 ppm. ESI (m/z): 1345.23 [2M + Na]$^+$, 1121.17 [2M-Phen], 723.13 [Au(PyPhos)$_2$]$^+$, 662.12 [M + H]$^+$, IR (cm^{-1}): ν = 3054.27 (ar), 2112.14 (C≡C), 1568.12 (C═N), 1478.04 (C−H), 1100.13 (P−C).

*[(PyPh$_2$P)$_4$Cu$_4$Au$_4$(C≡CPhen)$_4$][PF$_6$]$_4$ (**Cu2a**).* In a sealed flask under a N_2 atmosphere, **complex 2** (10 mg, 0.0178 mmol, 1 equiv) was added in 3 mL of CH_2Cl_2 under stirring for 5 min. Then, [Cu(MeCN)$_4$]PF$_6$ (6.09 mg, 0.0178 mmol, 1 equiv) dissolved in 2 mL of CH_2Cl_2 was added. After 3 h, the solution was reduced to dryness under vacuum. The solid was dissolved in 1 mL of dichloromethane and precipitated with 2 mL of hexane. **Cu2a** was obtained as a red-orange solid (9.6 mg, 82%). ^{1}H NMR: ($CDCl_3$, 400 MHz) δ = 9.35 (s, 1H), 8.56 (dd, J = 16.2, 7.8 Hz, 3H), 8.45 (d, J = 7.9 Hz, 2H), 8.07 (s, 2H), 7.78 (s, 1H), 7.60−7.65 (m, 3H). 7.62 (d, J = 7.6 Hz, 1H), 7.49 (dd, J = 15.2, 7.7 Hz, 1H), 7.39−7.29 (m, 3H), 7.05 (dd, J = 7.8 Hz, 1H), 6.74 (s, 1H), 6.44−6.25 (m, 4H) ppm; ^{19}F NMR: ($CDCl_3$ 162 MHz) δ = −73.65 ppm (d, J_{P-F} 712.0 Hz, 6F), ^{31}P NMR: ($CDCl_3$ 162 MHz) δ = 39.73 (s), −146.98 (hept) ppm. ESI (m/z): 2046.28 [3M + Cu + H]$^+$, 1483.07 [2M + 2Cu + Cl + H]$^+$, 1385.17 [2M + Cu + H]$^+$, 723.13 [Au(PyPhos)$_2$]$^+$, IR (cm^{-1}): ν

https://doi.org/10.1021/acs.inorgchem.3c00046
Inorg. Chem. XXXX, XXX, XXX−XXX

= 3057.16 (ar), 2005.33 (C≡C), 1584.29 (C═N), 1132.45 (P−C), 834.20 (P−F).

$[(PyPh_2P)_4Cu_4Au_4(C{\equiv}CPhen)_4][OTf]_4$ ***(Cu2b)***. In a sealed flask under a N_2 atmosphere, **complex 2** (10 mg, 0.0178 mmol, 1 equiv) was added in 3 mL of CH_2Cl_2 under stirring for 5 min. Then, $[Cu(MeCN)_4]OTf$ (6.09 mg, 0.0178 mmol, 1 equiv) dissolved in 2 mL of CH_2Cl_2 was added. After 3 h, the solution was reduced to dryness under vacuum. The solid was dissolved in 1 mL of dichloromethane and precipitated with 2 mL of hexane. **Cu2b** was obtained as a red-orange solid (10.1 mg, 88%). ^{1}H NMR: ($CDCl_3$, 400 MHz) δ = 9.37 (s, 1H), 8.59 (d, J = 9.1 Hz, 1H), 8.55 (d, J = 8.3 Hz, 1H), 8.53 (d, J = 7.1 Hz, 1H), 8.17 (s, 1H), 7.93−7.84 (m, 1H), 7.72−7.66 (m, 1H), 7.64 (t, J = 7.8 Hz, 1H), 7.55−7.44 (m, 1H), 7.43−7.31 (m, 8H), 7.06 (d, J = 11.5 Hz, 1H), 6.77 (s, 1H), 7.50−7.29 (m, 4H) ppm; ^{19}F NMR: ($CDCl_3$ 162 MHz) δ = −77.96 (s, 3F) ppm,^{31}P NMR: ($CDCl_3$ 162 MHz) δ = 39.91 (s) ppm. ESI (m/z): 2047.22 $[3M + Cu + H]^+$, 1485.06 $[2M + 2Cu + Cl + H]^+$, 1385.17 $[2M + Cu + H]^+$, 1121.17 $[2M + H]^+$ 723.13 $[Au(PyPhos)_2]^+$. IR (cm^{-1}): ν = 2961.97 (ar), 2005.52 (C≡C), 1524.67 (C═N), 1257.80 (CF_3), 1098.67 (P−C).

$[(PyPh_2P)_4Cu_4Au_4(C{\equiv}CPhen)_4][BF_4]_4$ ***(Cu2c)***. In a sealed flask under a N_2 atmosphere, **complex 2** (10 mg, 0.0178 mmol, 1 equiv) was added in 3 mL of CH_2Cl_2 under stirring for 5 min. Then, $[Cu(MeCN)_4]BF_4$ (6.09 mg, 0.0178 mmol, 1 equiv) dissolved in 2 mL of CH_2Cl_2 was added. After 3 h, the solution was reduced to dryness under vacuum. The solid was dissolved in 1 mL of dichloromethane and precipitated with 2 mL of hexane. **Cu2c** was obtained as a red-orange solid (8.3 mg, 77%). ^{1}H NMR: ($CDCl_3$, 400 MHz) δ = 9.36 (s, 1H), 8.59 (s, 1H), 8.54 (d, J = 8.3 Hz, 1H), 8.46 (d, J = 7.7 Hz, 2H), 8.14 (s, 2H), 7.89−7.80 (m, 1H), 7.70−7.65 (m, 3H), 7.63 (t, J = 7.7 Hz, 2H), 7.52−7.44 (m, 2H), 7.39−7.31 (m, 2H), 7.06 (d, J = 12.0 Hz, 1H), 7.66 (s, 1H), 7.46−7.29 (m, 4H) ppm; ^{19}F NMR: ($CDCl_3$ 162 MHz) δ = −153.43 ppm (s, 4F), ^{31}P NMR: ($CDCl_3$ 162 MHz) δ = 39.77 (s) ppm. ESI (m/z): 1483.07 $[2M + 2Cu + Cl + H]^+$, 1385.17 $[2M + Cu + H]^+$, 1121.17 $[M + Au + H]^+$, 723.13 $[Au(PyPhos)_2]^+$, IR (cm^{-1}): ν = 2905.04 (ar), 2077.07 (C≡C), 1584.96 (C═N), 1258.61 (B−F), 1012.17 (P−C).

■ ASSOCIATED CONTENT

Supporting Information

The Supporting Information is available free of charge at https://pubs.acs.org/doi/10.1021/acs.inorgchem.3c00046.

^{1}H and ^{31}P NMR spectra for all complexes; ESI-TOF spectra for all complexes; absorption and emission spectra for all compounds; X-ray crystal packing of **Cu1a**; absorption and emission spectra of all compounds in solution (air-equilibrated and N_2-saturated samples), solid and organic polymer matrices (PMMA and PS); emission lifetime data of all compounds; emission spectra for the calculation of singlet oxygen production; and crystal data and structure refinement for the **Cu1a**, **Cu2a**, and **Cu2c** (PDF)

Accession Codes

CCDC 2234334−2234336 contain the supplementary crystallographic data for this paper. These data can be obtained free of charge via www.ccdc.cam.ac.uk/data_request/cif, or by emailing data_request@ccdc.cam.ac.uk, or by contacting The Cambridge Crystallographic Data Centre, 12 Union Road, Cambridge CB2 1EZ, UK; fax: +44 1223 336033.

■ AUTHOR INFORMATION

Corresponding Author

Laura Rodríguez − *Departament de Química Inorgànica i Orgànica, Secció de Química Inorgànica, Universitat de Barcelona, 08028 Barcelona, Spain; Institut de Nanociència i Nanotecnologia (IN2UB), Universitat de Barcelona, 08028 Barcelona, Spain;* orcid.org/0000-0003-1289-1587; Email: laura.rodriguez@qi.ub.es

Authors

Guillermo Romo-Islas − *Departament de Química Inorgànica i Orgànica, Secció de Química Inorgànica, Universitat de Barcelona, 08028 Barcelona, Spain; Institut de Nanociència i Nanotecnologia (IN2UB), Universitat de Barcelona, 08028 Barcelona, Spain;* orcid.org/0000-0002-2841-9546

Jas S. Ward − *Department of Chemistry, University of Jyvaskyla, 40014 Jyvaskyla, Finland;* orcid.org/0000-0001-9089-9643

Kari Rissanen − *Department of Chemistry, University of Jyvaskyla, 40014 Jyvaskyla, Finland;* orcid.org/0000-0002-7282-8419

Complete contact information is available at: https://pubs.acs.org/10.1021/acs.inorgchem.3c00046

Notes

The authors declare no competing financial interest.

■ ACKNOWLEDGMENTS

The authors are grateful to Project PID2019-104121GB-I00 funded by the Ministerio de Ciencia e Innovación of Spain MCIN/AEI/10.13039/501100011033. G.R.-I. acknowledges Fundación Carolina and Secretaría de Relaciones Exteriores de México for the Ph.D. Scholarship.

■ REFERENCES

(1) Han, Z.; Zhao, X.; Peng, P.; Li, S.; Zhang, C.; Cao, M.; Li, K.; Wang, Z. Y.; Zang, S. Q. Intercluster Aurophilicity-Driven Aggregation Lighting Circularly Polarized Luminescence of Chiral Gold Clusters. *Nano Res.* **2020**, *13*, 3248−3252.

(2) Niermeier, P.; Wickemeyer, L.; Neumann, B.; Stammler, H. G.; Goett-Zink, L.; Kottke, T.; Mitzel, N. W. Aurophilicity in Action: Stepwise Formation of Dinuclear Au(I) Macrocycles with Rigid 1,8-Dialkynylanthracenes. *Dalton Trans.* **2019**, *48*, 4109−4113.

(3) Liu, C. Y.; Wei, X. R.; Chen, Y.; Wang, H. F.; Ge, J. F.; Xu, Y. J.; Ren, Z. G.; Braunstein, P.; Lang, J. P. Tetradecanuclear and Octadecanuclear Gold(I) Sulfido Clusters: Synthesis, Structures, and Luminescent Selective Tracking of Lysosomes in Living Cells. *Inorg. Chem.* **2019**, *58*, 3690−3697.

(4) Artem'ev, A. V.; Bagryanskaya, I. Y.; Doronina, E. P.; Tolstoy, P. M.; Gushchin, A. L.; Rakhmanova, M. I.; Ivanov, A. Y.; Suturina, A. O. A New Family of Clusters Containing a Silver-Centered Tetracapped [Ag@Ag4(M3-P)4] Tetrahedron, Inscribed within a N12 Icosahedron. *Dalton Trans.* **2017**, *46*, 12425−12429.

(5) Habermehl, N. C.; Eisler, D. J.; Kirby, C. W.; Yue, N. L. S.; Puddephatt, R. J. A Structural Probe for Organogold(I) Rings and [2]Catenanes. *Organometallics* **2006**, *25*, 2921−2928.

(6) Guo, P.; Jin, R.; Wang, M.; He, Q.; Cai, C.; Zhao, Q.; Bu, W. Chiral Gold(I)-Containing Polymeric Composites: Chiroptical Sensing and Circularly Polarized Luminescence. *J. Organomet. Chem.* **2021**, *931*, No. 121616.

(7) Ibáñez, S.; Poyatos, M.; Peris, E. Preparation and Self-Aggregation Properties of a Series of Pyrene-Imidazolylidene Complexes of Gold (I). *J. Organomet. Chem.* **2020**, *917*, No. 121284.

(8) Hong, E. Y. H.; Yam, V. W. W. Triindole-Tris-Alkynyl-Bridged Trinuclear Gold(I) Complexes for Cooperative Supramolecular Self-Assembly and Small-Molecule Solution-Processable Resistive Memories. *ACS Appl. Mater. Interfaces* **2017**, *9*, 2616−2624.

(9) Bowmaker, G. A.; Hanna, J. V.; King, S. P.; Marchetti, F.; Pettinari, C.; Pizzabiocca, A.; Skelton, B. W.; Sobolev, A. N.; Tebecaru, A.; White, A. H. Complexes of Copper(I) Thiocyanate with Monodentate Phosphine and Pyridine Ligands and the P(,N)-

Donor Diphenyl(2-Pyridyl)Phosphine. *Eur. J. Inorg. Chem.* **2014**, *2014*, 6104−6116.
(10) Busch, J. M.; Zink, D. M.; Di Martino-Fumo, P.; Rehak, F. R.; Boden, P.; Steiger, S.; Fuhr, O.; Nieger, M.; Klopper, W.; Gerhards, M.; Bräse, S. Highly Soluble Fluorine Containing Cu(I) AlkylPyrPhos TADF Complexes. *Dalton Trans.* **2019**, *48*, 15687−15698.
(11) Blanco, M. C.; Cámara, J.; Fernández-Moreira, V.; Laguna, A.; Gimeno, M. C. Gold(I), Phosphanes, and Alkynyls: The Perfect Allies in the Search for Luminescent Compounds. *Eur. J. Inorg. Chem.* **2018**, *2018*, 2762−2767.
(12) Yang, J.-S.; Zhang, M. M.; Han, Z.; Li, H. Y.; Li, L. K.; Dong, X. Y.; Zang, S. Q.; Mak, T. C. W. A New Silver Cluster That Emits Bright-Blue Phosphorescence. *Chem. Commun.* **2020**, *56*, 2451−2454.
(13) Cheng, E. C. C.; Lo, W. Y.; Lee, T. K. M.; Zhu, N.; Yam, V. W. W. Synthesis, Characterization, and Luminescence Studies of Discrete Polynuclear Gold(I) Sulfido and Selenido Complexes with Intramolecular Aurophilic Contacts. *Inorg. Chem.* **2014**, *53*, 3854−3863.
(14) Kayoko Itokazu, M.; Sarto Polo, A.; Murakami Iha, N. Y. Luminescent Rigidochromism of Fac-[Re(CO)3(Phen)(Cis-Bpe)]+ and Its Binuclear Complex as Photosensors Melina. *J. Photochem. Photobiol., A* **2003**, *160*, 27−32.
(15) Yang, X.; Wang, S.; Ghiviriga, I.; Abboud, K. A.; Veige, A. S. Organogold Oligomers: Exploiting iClick and Aurophilic Cluster Formation to Prepare Solution Stable Au4 Repeating Units. *Dalton Trans.* **2015**, *44*, 11437−11443.
(16) Huang, C. H.; Yang, M.; Chen, X. L.; Lu, C. Z. Bright Bluish-Green Emitting Cu(I) Complexes Exhibiting Efficient Thermally Activated Delayed Fluorescence. *Dalton Trans.* **2021**, *50*, 5171−5176.
(17) Artem'ev, A. V.; Shafikov, M.; Schinabeck, A.; Antonova, O. V.; Berezin, A. S.; Bagryanskaya, I. Y.; Plyusnin, P. E.; Yersin, H. Sky-blue Thermally Activated Delayed Fluorescence (TADF) Based on Ag(I) Complexes: Strong Solvation-Induced Emission Enhancement. *Inorg. Chem. Front.* **2019**, *6*, 3168−3176.
(18) Hofbeck, T.; Monkowius, U.; Yersin, H. Highly Efficient Luminescence of Cu(I) Compounds: Thermally Activated Delayed Fluorescence Combined with Short-Lived Phosphorescence. *J. Am. Chem. Soc.* **2015**, *137*, 399−404.
(19) Pinto, A.; Spigolon, G.; Gavara, R.; Zonta, C.; Licini, G.; Rodríguez, L. Tripodal Gold(i) Polypyridyl Complexes and Their Cu +and Zn2+ heterometallic Derivatives. Effects on Luminescence. *Dalton Trans.* **2020**, *49*, 14613−14625.
(20) de Aquino, A.; Caparrós, F. J.; Aullón, G.; Truong, K. N.; Rissanen, K.; Lima, J. C.; Rodríguez, L. Development of Gold(I) Phosphorescent Tweezers for Sensing Applications. *Dalton Trans.* **2022**, *51*, 16282−16291.
(21) Caparrós, F. J.; Outis, M.; Jung, Y.; Choi, H.; Lima, J. C.; Rodríguez, L. Luminescent Tetranuclear Gold(I) Dibenzo[g,p]-Chrysene Derivatives: Effect of the Environment on Photophysical Properties. *Molecules* **2020**, *25*, No. 949.
(22) Pinto, A.; Svahn, N.; Lima, J. C.; Rodríguez, L. Aggregation Induced Emission of Gold(I) Complexes in Water or Water Mixtures. *Dalton Trans.* **2017**, *46*, 11125−11139.
(23) Moro, A. J.; Avó, J.; Malfois, M.; Zaccaria, F.; Fonseca Guerra, C.; Caparrós, F. J.; Rodríguez, L.; Lima, J. C. Aggregation Induced Emission of a New Naphthyridine-Ethynyl-Gold(I) Complex as a Potential Tool for Sensing Guanosine Nucleotides in Aqueous Media. *Dalton Trans.* **2020**, *49*, 171−178.
(24) Aguiló, E.; Moro, A. J.; Gavara, R.; Alfonso, I.; Pérez, Y.; Zaccaria, F.; Guerra, C. F.; Malfois, M.; Baucells, C.; Ferrer, M.; Lima, J. C.; Rodríguez, L. Reversible Self-Assembly of Water-Soluble Gold(I) Complexes. *Inorg. Chem.* **2018**, *57*, 1017−1028.
(25) Pujadas, M.; Rodríguez, L. Luminescent Phosphine Gold(I) Alkynyl Complexes. Highlights from 2010 to 2018. *Coord. Chem. Rev.* **2020**, *408*, No. 213179.
(26) Lima, J. C.; Rodríguez, L. Applications of Gold(I) Alkynyl Systems: A Growing Field to Explore. *Chem. Soc. Rev.* **2011**, *40*, 5442−5456.
(27) Donamaría, R.; Lippolis, V.; López-De-Luzuriaga, J. M.; Monge, M.; Nieddu, M.; Olmos, M. E. Influence of the Number of Metallophilic Interactions and Structures on the Optical Properties of Heterometallic Au/Ag Complexes with Mixed-Donor Macrocyclic Ligands. *Inorg. Chem.* **2018**, *57*, 11099−11112.
(28) Laguna, A. In *Modern Supramolecular Gold Chemistry*; Laguna, A., Ed.; Wiley-VCH Verlag GmbH & Co. KGaA: Weinheim, Germany, 2008.
(29) Schmidbaur, H.; Schier, A. A Briefing on Aurophilicity. *Chem. Soc. Rev.* **2008**, *37*, 1931−1951.
(30) Pinto, A.; Hernández, G.; Gavara, R.; Aguiló, E.; Moro, A. J.; Aullón, G.; Malfois, M.; Lima, J. C.; Rodríguez, L. Supramolecular Tripodal Au(I) Assemblies in Water. Interactions with a Pyrene Fluorescent Probe. *New J. Chem.* **2019**, *43*, 8279−8289.
(31) Pinto, A.; Svahn, N.; Lima, J. C.; Rodríguez, L. Aggregation Induced Emission of Gold(I) Complexes in Water or Water Mixtures. *Dalton Trans.* **2017**, *46*, 11125−11139.
(32) Cunha, C.; Pinto, A.; Galva, A.; Rodríguez, L.; Seixas de Melo, J. S. Aggregation-Induced Emission with Alkynylcoumarin Dinuclear Gold(I) Complexes: Photophysical, Dynamic Light Scattering, and Time-Dependent Density Functional Theory Studies˜. *Inorg. Chem.* **2022**, *61*, 6964−6976.
(33) Yam, V. W.; Wong, K. M.; Wong, K. M.; Wong, K. M. ChemComm Luminescent Metal Complexes of d^6, d^8 and d^{10} Transition Metal Centres. *Chem. Commun.* **2011**, *47*, 11579−11592.
(34) Nayeri, S.; Jamali, S.; Jamjah, A.; Shakirova, J. R.; Tunik, S. P.; Gurzhiy, V.; Samouei, H.; Shahsavari, H. R. Five- And Six-Coordinated Silver(I) Complexes Formed by a Metallomacrocyclic Ligand with a "Au2N2" Donor Group: Observation of Pendulum and Linear Motions and Dual Phosphorescence. *Inorg. Chem.* **2020**, *59*, 5702−5712.
(35) Shakirova, J. R.; Grachova, E. V.; Gurzhiy, V. V.; Thangaraj, S. K.; Jänis, J.; Melnikov, A. S.; Karttunen, A. J.; Tunik, S. P.; Koshevoy, I. O. Heterometallic Cluster-Capped Tetrahedral Assemblies with Postsynthetic Modification of the Metal Cores. *Angew. Chem., Int. Ed.* **2018**, *57*, 14154−14158.
(36) Hernández-Toledo, H.; Torrens, H.; Flores-Álamo, M.; De Cola, L.; Moreno-Alcántar, G. Self-Assembly and Aggregation-Induced Emission in Aqueous Media of Responsive Luminescent Copper(I) Coordination Polymer Nanoparticles. *Chem.—Eur. J.* **2021**, *27*, 8308−8314.
(37) Dayanova, I. R.; Shamsieva, A. V.; Strelnik, I. D.; Gerasimova, T. P.; Kolesnikov, I. E.; Fayzullin, R. R.; Islamov, D. R.; Saifina, A. F.; Musina, E. I.; Hey-Hawkins, E.; Karasik, A. A. Assembly of Heterometallic AuICu2I2Cores on the Scaffold of NPPN-Bridging Cyclic Bisphosphine. *Inorg. Chem.* **2021**, *60*, 5402−5411.
(38) Malpicci, D.; Lucenti, E.; Forni, A.; Marinotto, D.; Previtali, A.; Carlucci, L.; Mercandelli, P.; Botta, C.; Righetto, S.; Cariati, E. Ag(I) and Cu(I) Cyclic-Triimidazole Coordination Polymers: Revealing Different Deactivation Channels for Multiple Room Temperature Phosphorescences. *Inorg. Chem. Front.* **2021**, *8*, 1312−1323.
(39) DeRosa, M. C.; Crutchley, R. J. Photosensitized Singlet Oxygen and Its Applications. *Coord. Chem. Rev.* **2002**, *233*−*234*, 351−371.
(40) Zhu, Z.; Tang, Z.; Phillips, J. A.; Yang, R.; Wang, H.; Tan, W. Regulation of Singlet Oxygen Generation Using Single-Walled Carbon Nanotubes. *J. Am. Chem. Soc.* **2008**, *130*, 10856−10857.
(41) Ge, J.; Lan, M.; Zhou, B.; Liu, W.; Guo, L.; Wang, H.; Jia, Q.; Niu, G.; Huang, X.; Zhou, H.; Meng, X.; Wang, P.; Lee, C. S.; Zhang, W.; Han, X. A Graphene Quantum Dot Photodynamic Therapy Agent with High Singlet Oxygen Generation. *Nat. Commun.* **2014**, *5*, No. 4596.
(42) Hirakawa, K.; Hirano, T.; Nishimura, Y.; Arai, T.; Nosaka, Y. Dynamics of Singlet Oxygen Generation by DNA-Binding Photosensitizers. *J. Phys. Chem. B* **2012**, *116*, 3037−3044.
(43) Kim, S.; Tachikawa, T.; Fujitsuka, M.; Majima, T. Far-Red Fluorescence Probe for Monitoring Singlet Oxygen during Photodynamic Therapy. *J. Am. Chem. Soc.* **2014**, *136*, 11707−11715.
(44) Li, Z.; Chen, S.; Huang, Y.; Zhou, H.; Yang, S.; Zhang, H.; Wang, M.; Guo, H.; Yin, J. Photoswitchable AIE Photosensitizer for Reversible Control of Singlet Oxygen Generation in Specific Bacterial

https://doi.org/10.1021/acs.inorgchem.3c00046
Inorg. Chem. XXXX, XXX, XXX−XXX

Discrimination and Photocontrolled Photodynamic Killing of Bacteria. *Chem. Eng. J.* **2022**, *450*, No. 138087.
(45) Zhang, S.; Li, Y.; Li, T.; Zhang, Y.; Li, H.; Cheng, Z.; Peng, N.; Liu, Y.; Xu, J.; He, H. Activable Targeted Protein Degradation Platform Based on Light-Triggered Singlet Oxygen. *J. Med. Chem.* **2022**, *65*, 3632−3643.
(46) Ma, W.; Mao, J.; He, C. T.; Shao, L.; Liu, J.; Wang, M.; Yu, P.; Mao, L. Highly Selective Generation of Singlet Oxygen from Dioxygen with Atomically Dispersed Catalysts. *Chem. Sci.* **2022**, *13*, 5606−5615.
(47) Sharma, B.; Jain, A.; Pérez-García, L.; Watts, J. A.; Rawson, F. J.; Chaudhary, G. R.; Kaur, G. Metallocatanionic Vesicle-Mediated Enhanced Singlet Oxygen Generation and Photodynamic Therapy of Cancer Cells. *J. Mater. Chem. B* **2022**, *10*, 2160−2170.
(48) Younis, M. R.; He, G.; Qu, J.; Lin, J.; Huang, P.; Xia, X. H. Inorganic Nanomaterials with Intrinsic Singlet Oxygen Generation for Photodynamic Therapy. *Adv. Sci.* **2021**, *8*, No. 2102587.
(49) Fales, A. M.; Yuan, H.; Vo-Dinh, T. Silica-Coated Gold Nanostars for Combined Surface-Enhanced Raman Scattering (SERS) Detection and Singlet-Oxygen Generation: A Potential Nanoplatform for Theranostics. *Langmuir* **2011**, *27*, 12186−12190.
(50) Tamtaji, M.; Kazemeini, M. Utilizing Graphene Oxide/Gold/Methylene Blue Ternary Nanocomposite as a Visible Light Photocatalyst for a Plasmon-Enhanced Singlet Oxygen Generation. *React. Kinet. Mech. Catal.* **2022**, *135*, 2851−2865.
(51) Üçüncü, M.; Karakuş, E.; Kurulgan Demirci, E.; Sayar, M.; Dartar, S.; Emrullahoglu, M. BODIPY-Au(I): A Photosensitizer for Singlet Oxygen Generation and Photodynamic Therapy. *Org. Lett.* **2017**, *19*, 2522−2525.
(52) Sahu, K.; Angeloni, S.; Conradie, J.; Villa, M.; Nayak, M.; Ghosh, A.; Ceroni, P.; Kar, S. NIR-Emissive, Singlet-Oxygen-Sensitizing Gold Tetra(Thiocyano)Corroles. *Dalton Trans.* **2022**, *51*, 13236−13245.
(53) Pinto, A.; Cunha, C.; Aullón, G.; Lima, J. C.; Rodríguez, L.; Seixas de Melo, J. S. Comprehensive Investigation of the Photophysical Properties of Alkynylcoumarin Gold(I) Complexes. *J. Phys. Chem. B* **2021**, *125*, 11751−11760.
(54) Pinto, A.; Ward, J. S.; Rodríguez, L.; Rissanen, K.; Smith, M. Aggregation of Gold(I) Complexes: Phosphorescence vs. Singlet Oxygen Production. *Dalton Trans.* **2022**, *51*, 8795−8803.
(55) Petrovskii, S. K.; Paderina, A. V.; Sizova, A. A.; Baranov, A. Y.; Artem'ev, A. A.; Sizov, V. V.; Grachova, E. V. Luminescence Behaviour of Au(I)-Cu(I) Heterobimetallic Coordination Polymers Based on Alkynyl-Tris(2-Pyridyl)Phosphine Au(i) Complexes. *Dalton Trans.* **2020**, *49*, 13430−13439.
(56) Nayeri, S.; Jamali, S.; Jamjah, A.; Samouei, H. Tetranuclear Au2Cu2 Clusters with Butterfly- And Planar-Shaped Metal Cores: Strong Rigidochromism Induced by Jahn-Teller Distortion in Two-Coordinated Gold(I) Centers. *Inorg. Chem.* **2019**, *58*, 12122−12131.
(57) Jiang, Y.; Guo, W. J.; Kong, D. X.; Wang, Y. T.; Wang, J. Y.; Wei, Q. H. Novel Electrochemi-/Photo-Luminescence of Ag3Cu5 Heterometallic Alkynyl Clusters. *Dalton Trans.* **2015**, *44*, 3941−3944.
(58) Moro, A. J.; Rome, B.; Aguiló, E.; Arcau, J.; Puttreddy, R.; Rissanen, K.; Lima, J. C.; Rodríguez, L. A Coumarin Based Gold(I)-Alkynyl Complex: A New Class of Supramolecular Hydrogelators. *Org. Biomol. Chem.* **2015**, *13*, 2026−2033.
(59) Gavara, R.; Llorca, J.; Lima, J. C.; Laura, R. A Luminescent Hydrogel Based on a New Au(I) Complex. *Chem. Commun.* **2013**, *49*, 72−74.
(60) Rosental, M.; Coldman, R. N.; Moro, A. J.; Angurell, I.; Gomila, R. M.; Frontera, A.; Lima, J. C.; Rodríguez, L. Using Room Temperature Phosphorescence of Gold (I) Complexes for PAHs Sensing. *Molecules* **2021**, *26*, No. 2444.
(61) Ang, H. G.; Kow, W. E.; Mok, K. F. Metallic complexes of 2.pyridyldiphosphine. *Inorg. Nucl. Chem. Lett.* **1972**, *8*, 829−832.
(62) Vícha, J.; Novotny, J.; Komorovsky, S.; Straka, M.; Kaupp, M.; Marek, R. Relativistic Heavy-Neighbor-Atom E Ff Ects on NMR Shifts: Concepts and Trends Across the Periodic Table. *Chem. Rev.* **2020**, *120*, 7065−7103.
(63) Novotný, J.; Jan, V.; Bora, P. L.; Repisky, M.; Straka, M.; Komorovsky, S.; Marek, R. Linking the Character of the Metal − Ligand Bond to the Ligand NMR Shielding in Transition-Metal Complexes: NMR Contributions from Spin − Orbit Coupling. *J. Chem. Theory Comput.* **2017**, *13*, 3586−3601.
(64) Blanco, M. C.; Cámara, J.; Gimeno, M. C.; Laguna, A.; James, S. L.; Lagunas, M. C.; Villacampa, M. D. Synthesis of Gold-Silver Luminescent Honeycomb Aggregates by Both Solvent-Based and Solvent-Free Methods. *Angew. Chem., Int. Ed.* **2012**, *51*, 9777−9779.
(65) Yam, V. W. W.; Au, V. K. M.; Leung, S. Y. L. Light-Emitting Self-Assembled Materials Based on d^8 and d^{10} Transition Metal Complexes. *Chem. Rev.* **2015**, *115*, 7589−7728.
(66) Mondal, R.; Lozada, I. B.; Davis, R. L.; Williams, J. A. G.; Herbert, D. E. Exploiting Synergy between Ligand Design and Counterion Interactions to Boost Room Temperature Phosphorescence from Cu(I) Compounds. *J. Mater. Chem. C* **2019**, *7*, 3772−3778.
(67) Shakirova, J. R.; Grachova, E. V.; Gurzhiy, V. V.; Koshevoy, I. O.; Melnikov, A. S.; Sizova, O. V.; Tunik, S. P.; Laguna, A. Luminescent Heterometallic Gold-Copper Alkynyl Complexes Stabilized by Tridentate Phosphine. *Dalton Trans.* **2012**, *41*, 2941−2949.
(68) Schäfer, S.; Gamer, M. T.; Lebedkin, S.; Weigend, F.; Kappes, M. M.; Roesky, P. W. Bis(6-Methylene-2,2′-Bipyridine)-Phenylphosphine—A Flexible Ligand for the Construction of Trinuclear Coinage-Metal Complexes. *Chem.—Eur. J.* **2017**, *23*, 12198−12209.
(69) Koshevoy, I. O.; Lin, Y. C.; Karttunen, A. J.; Chou, P. T.; Vainiotalo, P.; Tunik, S. P.; Haukka, M.; Pakkanen, T. A. Intensely Luminescent Alkynyl - Phosphine Gold(l) - Copper(l) Complexes: Synthesis, Characterization, Photophysical, and Computational Studies. *Inorg. Chem.* **2009**, *48*, 2094−2102.
(70) Crespo, O.; Gimeno, M. C.; Laguna, A.; Lahoz, F. J.; Larraz, C. Unprecedented Luminescent Heteropolynuclear Aggregates with Gold Thiolates as Building Blocks. *Inorg. Chem.* **2011**, *50*, 9533−9544.
(71) Lei, Z.; Pei, X. L.; Guan, Z. J.; Wang, Q. M. Full Protection of Intensely Luminescent Gold(I)−Silver(I) Cluster by Phosphine Ligands and Inorganic Anions. *Angew. Chem., Int. Ed.* **2017**, *56*, 7117−7120.
(72) Catalano, V. J.; López-De-Luzuriaga, J. M.; Monge, M.; Olmos, M. E.; Pascual, D. Copper(I)-Assisted Red-Shifted Phosphorescence in Au(I)···Cu(I) Heteropolynuclear Complexes. *Dalton Trans.* **2014**, *43*, 16486−16497.
(73) Han, Z.; Si, Y.; Dong, X. Y.; Hu, J. H.; Zhang, C.; Zhao, X. H.; Yuan, J. W.; Wang, Y.; Zang, S. Q. Smart Reversible Transformations between Chiral Superstructures of Copper Clusters for Optical and Chiroptical Switching. *J. Am. Chem. Soc.* **2023**, *145*, 6166−6176.
(74) Gusev, A.; Kiskin, M.; Braga, E.; Zamnius, E.; Kryukova, M.; Karaush-Karmazin, N.; Baryshnikov, G.; Minaev, B.; Linert, W. Structure and Emission Properties of Dinuclear Copper(I) Complexes with Pyridyltriazole. *RSC Adv.* **2023**, *13*, 3899−3909.
(75) Pinto, A.; Echeverri, M.; Gómez-Lor, B.; Rodríguez, L. Dyes and Pigments How to Achieve near Unity Fluorescence Quantum Yields on Gold (I) Benzothiadiazole-Based Derivatives. *Dyes Pigm.* **2022**, *202*, No. 110308.
(76) Uson, R.; Laguna, A.; Laguna, M.et al.(Tetrahydrothiophene)-Gold(I) or Gold(III) Complexes. *Inorganic Syntheses*; John Wiley & Sons, Inc., 1989; Vol. *6*, pp 85−91.
(77) Sheldrick, G. M. SHELXT - Integrated Space-Group and Crystal-Structure Determination. *Acta Crystallogr., Sect. A: Found. Adv.* **2015**, *71*, 3−8.
(78) Dolomanov, O. V.; Bourhis, L. J.; Gildea, R. J.; Howard, J. A. K.; Puschmann, H. OLEX2: A Complete Structure Solution, Refinement and Analysis Program. *J. Appl. Crystallogr.* **2009**, *42*, 339−341.
(79) Sheldrick, G. M. Crystal Structure Refinement with SHELXL. *Acta Crystallogr., Sect. C: Struct. Chem.* **2015**, *71*, 3−8.

https://doi.org/10.1021/acs.inorgchem.3c00046
Inorg. Chem. XXXX, XXX, XXX−XXX